Catalysis Letters (2018) 148:1181–1189
https://doi.org/10.1007/s10562-017-2292-1

Identification and Characterization of a Novel Halohydrin Dehalogenase from *Bradyrhizobium erythrophlei* and Its Performance in Preparation of Both Enantiomers of Epichlorohydrin

Feng Xue[1,2] · Jian Gao[1] · Li Zhang[1] · Han Li[1] · He Huang[2]

Received: 27 October 2017 / Accepted: 26 December 2017 / Published online: 17 February 2018

Abstract

The new halohydrin dehalogenase-like gene (HheB8) in the genome of *Bradyrhizobium erythrophlei* was identified, synthesized and expressed in *Escherichia coli*. The encoded protein (HheB8) was purified to homogeneity as a molecular mass of 26 kDa and characterized using the model substrate of 1,3-dicholoro-2-propanol (1,3-DCP). The purified HheB8 was optimally active at pH 9.5 and 45 °C, and highly stable at pH 6.0–8.0 and 40 °C or below. The enzyme displayed a very broad substrate specificity, exhibiting good enantioselectivity for the transformation of prochiral 1,3-DCP and 1,3-dibromo-2-propanol to (*R*)-ECH (92.3% enantiomeric excess *ee*) and (*R*)-epibromohydrin (81.3% *ee*). For all tested epoxides, except styrene oxide, the (*R*)-enantiomer was converted first, affording (*S*)-isomer in 99% *ee*. Furthermore, the potential for using a single HHDH to enantioselectively produce both enantiomers of ECH was analyzed. The bioconversion process for production of (*R*)-ECH from 1,3-DCP by the recombinant HheB8 was developed and a maximum *ee* of 93.4% was achieved. Kinetically resolved racemic ECH (30 mM) to provide (*S*)-ECH with 99% *ee* and 33.4% yield. To the best of our knowledge, this is the first report of HheB8 used as biocatalyst in the production of enantiopure ECH. Therefore, this recombinant HHDH could be a potential candidate for application in the synthesis of chiral chemicals from prochiral halohydrins and racemic epoxides.

Graphical Abstract

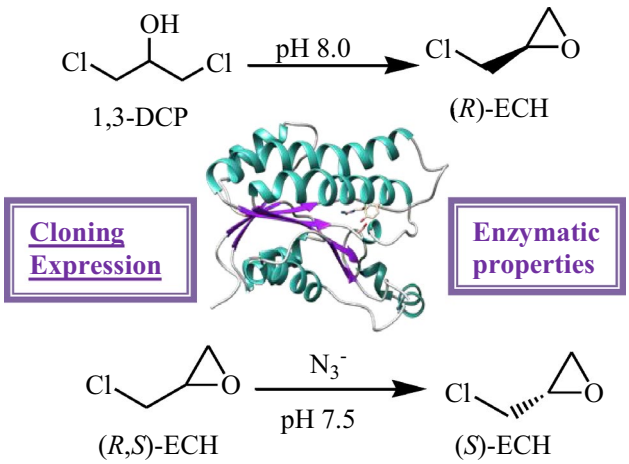

Keywords Enzymatic characteristics · Halohydrin dehalogenase · Enantiopure epichlorohydrin · Enantioselectivity

Extended author information available on the last page of the article

1 Introduction

Halohydrin dehalogenases (HHDHs, EC 4.5.1.X) are microbial enzymes that catalyze the conversion of vicinal haloalcohols to the corresponding epoxide, a proton and a halide ion. Alternatively, they can accept different anionic nucleophiles such as azide, cyanide, and nitrite, to open the epoxide ring [1]. Sequence and structure analysis showed that the catalytic mechanism of halohydrin dehalogenases is similar to that of members of the SDR superfamily of proteins. Both the SDR and HHDH enzymes present a conserved Ser/Tyr/Arg (or Ser/Tyr/Lys) catalytic triad, which participated in the abstraction of proton from the substrate hydroxyl group [2].

A quantity of halogenated organic chemicals are environmentally harmful industrial by-products, and it has been found that HHDHs may be competent catalysts for the potential uses in the bioremediation [2–4]. Recently, these HHDHs have attracted wide attention for their ability to produce various epoxides, β-substituted alcohols and halohydrins [1, 5–9]. Chiral epichlorohydrin (ECH) is a crucial intermediate for the preparation of β-blockers, atorvastatin, ferroelectric liquid crystals and L-carnitine [10]. Several different synthetic approaches including biological and chemical methods have been explored for the synthesis of this product. Enantioselective ring-opening reaction of racemic ECH with the nucleophiles catalyzed by HHDHs is a potential route to give optically active ECH [11]. A drawback of optical resolution method based on enantioselective resolution is that the desired enantiomer's yield is $< 50\%$. Stereoselective conversion of prochiral 1,3-dicholoro-2-propanol (1,3-DCP) using HHDH, which has been reported previously and could provide an alternative approach for the preparation of enantiopure ECH [12]. It is more advantageous than resolution techniques in which the theoretical yield of the chiral product is 100%.

HHDHs have generally been separated from bacteria colonizing environments contaminated with a halogenated aromatic compound [3, 13, 14]. In spite of a great number of studies to deal with the isolation of microbial strains exhibiting HHDH activity and purification of the corresponding enzymes, only a limited number of the genes encoding HHDHs have been cloned and characterized in detail [15–21]. Owing to the rapidly accumulation of genome sequencing data and the recent advances in bioinformatics, it is possible to acquire new HHDHs by data mining of genome sequence and analysis of potential HHDHs sequence and activity information. Recently, Schallmey report the strategy for identifying new HHDHs in freely available protein sequence databases by using specific sequence motifs which allow for the clear distinction between the large number of other SDR sequences and true HHDH sequences [22]. With the help of two conserved sequence motifs containing the nucleophile binding pocket (TX_4[FY]XG) and catalytic triad ($SX_{12}YX_3R$) architecture, it will be much faster and highly effective to identify novel HHDH enzymes in comparison to more time-consuming traditional microbiology and molecular biology techniques [22]. At the same time, only a few of these HHDHs have been obtained through recombinant techniques and hence it is of universal interest to explore the kinds of these enzymes to broaden their biocatalytic applications [23, 24].

In this study, a putative HHDH from *Bradyrhizobium erythrophlei* was identified by a Blast search of SDR superfamily. Although sequence of HheB8 from *B. erythrophlei* is annotated as "short-chain dehydrogenase", it is very likely to stand for a true HHDH enzyme since it possess a conserved catalytic triad of "S-x(12)-Y-x(3)-R". Here, we firstly reported the gene cloning, over-expression, and functional characterization of a novel HHDH with better enantioselectivities toward halohydrins and epoxides, which is a promising alternative for the production of chiral epichlorohydrin.

2 Materials and Methods

2.1 Chemicals

1,3-DCP, 2,3-DCP, 1,3-dibromo-2-propanol, 3-chloro-1,2-propanediol, (*R,S*)-ECH, (*S*)-ECH, (*R*)-ECH, styrene oxide and glycidyl phenyl ether were purchased from Sigma-Aldrich Chemical Co. (St. Louis, MO, USA). Isopropyl-d-thiogalactoside (IPTG) was from TaKaRa Biotechnology (Dalian, China). The pGEM-T (Promega, Madison, WI, USA) and pET28a (Novagen, Darmstadt, Germany) were used as cloning and expression vector, respectively. All the organic compounds were of reagent grade and were obtained from commercial sources.

2.2 Strains and Growth Condition

Escherichia coli JM 109 (Tiangen biotech Co., Ltd., Beijing, China) and *E. coli* BL21 (DE3) (Invitrogen, Karlsruhe, Germany) were used for gene cloning and gene expression, respectively. The *E. coli* strains were routinely cultured at 37 °C in Luria–Bertani (LB) medium, and supplemented with the appropriate antibiotic(s) [kanamycin (50 μg/mL)].

2.3 Gene Synthesis and Cloning

The HheBe gene was synthesized artificially according to the sequence deposited in the NCBI Protein database under accession number WP_079568045. The codon usage was automatically adapted to the codon bias of *E. coli*

genes by Mr. Gene's website service. For expression purposes, the gene was subcloned to the expression vector pET28a between restriction sites *Nco*I and *Xho*I. According to the manufacturer's instructions, the recombinant plasmid was transformed into the *E. coli* strain BL21(DE3) for protein overexpression.

2.4 Enzyme Production and Purification

To prepare recombinant HheB8, *E. coli* BL21 (DE3) cells harboring the pET28a–HheBe were grown at 37 °C in LB broth containing 50 μg/mL Kan until the optical density (OD) reached 0.8 at 600 nm. Then, IPTG was added at 0.1 mM and growth was carried out at 28 °C for extra 10 h. Cells were harvested by centrifugation for 10 min at 4 °C and 10,000×*g*, and re-suspended in 20 mM Tris–SO_4 buffer (pH 8.0). After disrupted by sonication for 15 min and removing the cell debris by centrifugation at 10,000×*g* for 10 min, the crude cell extract was filtered and applied to a nickel–nitrilotriacetic acid (Ni–NTA) column preequilibrated with Tris–SO_4 buffer (20 mM, pH 8.0). After washed with washing buffer [20 mM Tris–SO_4 (pH 8.0), 20 mM imidazole and 400 mM NaCl], the bound protein was eluted with elution buffer [20 mM Tris–SO_4 (pH 8.0), 400 mM imidazole and 400 mM NaCl], and then dialyzed overnight in ice with buffer containing 20 mM Tris–SO_4 (pH 8.0). The purified enzyme was collected for subsequent enzymatic characterization experiments. Using bovine serum albumin (BSA) as the standard, the enzyme content was determined by Bradford method [25]. 12% Sodium dodecyl sulfate polyacrylamide gel electrophoresis (SDS-PAGE) was applied for the determination of the molecular weight of the denatured protein with Coomassie brilliant blue G-250 [26].

2.5 Sequence Analysis and Homology Modeling

Sequence similarity searches were carried out using blastn and blastp, respectively. Sequence analyses were performed using ExPASy [27]. A multiple alignment of HHDH amino acid sequences from various microorganisms were constructed with software Clustalx 1.8.3 and decorated using the ESPript 3.0 network station for better visual effect [28]. The three-dimensional (3-D) structure of HheB8 was modeled by the Modeller 9.18 program using the crystal structure of HheB from *Corynebacterium* sp. strain N-1074 (PDB accession no. 4zd6) [29]. After further energy minimization, the quality of the final structure model was evaluated using the Procheck program. The modeled 3-D structure of HheB8 was visualized using the PyMOL and Chimera 1.9 software.

2.6 Analytical Methods

The concentration of various halohydrins and epichlorohydrin (ECH) in the reaction mixture was determined by Agilent 6890N GC system equipped with a HP-5 capillary column with N_2 as carrier gas [18]. The glycidyl azide and benzyl glycidyl ether was separated on a Chiralcel OD-H (Daicel Co., Japan; 4.6 × 250 mm). The mobile phase was n-hexane/isopropanol (8/2 and 9/1 v/v) at 0.8 mL/min [30]. ECH and SO were separated by chiral phase GC using a BGB-175 column [9]. According to the approach described by Chen et al., the value of ee_s (expressed as enantiomeric excess of the remaining epoxide) were calculated using the following equation: $ee_s = ([R] - [S])/([R] + [S])$ [31]. One unit (U) of HHDH activity was defined as the amount of enzyme that convert 1 μmol ECH or 1 μmol 1,3-DCP per minute under the assay conditions.

2.7 Enzymatic Properties of HheB8

The effects of temperature, pH and reagents on the catalytic activities were investigated. The optimal reaction pH was analyzed in 100 mM buffers as follows: sodium phosphate buffer (6.0–8.0), Tris–SO_4 buffer (7.0–8.5) and glycine–NaOH buffer (pH 8.0–10.5). The effect of temperature on the HheB8 activity was studied in the temperature between 20 and 60 °C in 0.1 M Tris–SO_4 buffer (pH 8.0). After pre-incubation for 30 min at temperatures ranging from 20 to 60 °C, the residual activity of the HheB8 was determined under standard conditions and unheated enzyme was used as a control (100%).

To map substrate scopes of this newly mined HHDH, its activity and enantioselectivity towards seven different halohydrins as well as five different epoxides was determined by monitoring epoxide ring closing or opening reaction. Analytical-scale dehalogenation reactions were performed in 2 mL Eppendorf tubes containing 400 μL Tris–SO_4 buffer (100 mM, pH 8.0), 20 mM halohydrins and an appropriate amount of the enzyme at 35 °C with a thermoshaker 400 rpm. Relative activity towards each halohydrins was measured by taking the 1,3-DCP as 100%. The epoxide ring-opening reactions were carried out at a 400 μL scale in 2 mL Eppendorf tubes with 30 mM sodium azide and 10 mM epoxides in 100 mM Tris–SO_4 buffer (pH 7.5). Temperature was kept at 30 °C, and the mixture was incubated in a thermoshaker at 400 rpm. Negative controls contained only sodium azide and substrate in buffer. The values were compared to the enzyme activity in the ECH solution. The HheB8 activity was determine as described above.

The influences of various metal ions, chelating agent EDTA, and surfactants on the HheB8 activity were investigated by using 1,3-DCP as the substrate in the reaction.

Relative activity was calculated as a percentage of the activity without any test compound.

2.8 Biocatalytic Formation of Enantiopure ECH by Whole Cells of Recombinant *E. coli*

The preparation of optically pure ECH from 1,3-DCP was investigated. The freshly prepared *E. coli* (HheBe) cell pellets were resuspended in 10 mL of 100 mM Gly–NaOH buffer, then 1,3-DCP was added, and the mixed solution were shaken at 180 rpm and 35 °C. Enantioselective hydrolysis of ECH in the presence of sodium azide as nucleophile were implemented in 100 mM Tris–SO_4 buffer (pH 7.5). For the biotransformation of 1,3-DCP and racmic ECH, 400 µL aliquots were taken out from the reaction solutions at different points of time. After centrifugation at 10,000×*g* for 4 min, the supernatant was extracted with ethyl acetate, dryed over Na_2SO_4, filtered, and analyzed by chiral GC to determine the *ee* and conversion, respectively.

2.9 Statistical Analysis

All data were reported as the means of triplicate experiments if not specifically noted. Analysis of variance (ANOVA) was carried out using the Statistical Analysis System (SAS) program version 8.1. The results are expressed as mean ± standard deviation (SD) and the least significant differences for comparison of means were computed at $p < 0.05$. All the figures presented in this study were drawn using the origin software version 8.0.

2.10 Sequence Submission

The encoding sequence has been deposited in the GenBank database with an accession number of MG251386.

3 Results and Discussion

3.1 Sequence Analysis of HheB8

Using the protein sequences of the known HHDHs as queries, Blast search of the nr database of GenBank led us to a gene of interest, having putative HHDH property. The deduced sequence of HheB8 having 675 bp, encoding 224 aa with the calculated molecular weight 24,251 Da and the theoretical isoelectric point 5.25, showed the characteristics of HHDH like "S-x(12)-Y-x(3)-R" motif with the catalytic triad ser^{115}–Tyr^{128}–Arg^{131}. Multiple sequence alignment of the HheB8 and several other known bacterial HHDH revealed its closest homology (56%) with HheB5 (GenBank accession no. KU501241) [24]. And it was 52, 49, 43, 31, 31 and 30%, identical to HheB7 (AMQ13564) from *Bradyrhizobium* sp., HheB (BAA14362) from *Corynebacterium* sp. strain N-1074, HHDH-Pl (ABS64560) from *Parvibaculum lavamentivorans* DS-1, HheA (BAA14361) from *Corynebacterium* sp. strain N-1074, HheC (AAK92099) from *Agrobacterium radiobacter* strain AD1, and $HHDH_{Tm}$ (AKR76215.1) from *Tistrella mobilis* ZJB1405 (Fig. 1). Three dimensional structure of HheB8 (Fig. 2) was predicted using the Modeller 9.18 based on the crystal structure of the HheB from *Corynebacterium* strain N-1074 (PDB accession no. 4zd6, 49% identity) as the closest template. Figure 2 shows that HheBe consists of a six stranded parallel β-sheet that is surrounded by eight α-helices. The stereochemical quality of the predicted protein structure was assessed by Procheck, it showed that 92.7% of the residues were located in the most favored regions of the Ramachandran diagram, 6.7% were present in the additionally allowed regions, while none of residues was observed in the disallowed regions. These results indicate that the model was reliable.

3.2 HHDH Expression and Purification

In order to express the HheB8, gene *hheB8* was subcloned into the expression vector pET28a(+) to construct the recombinant plasmid pET28a(+)–HheB8 and transformed into *E. coli* BL21(DE3). To facilitate the rapid purification, a His-tag was introduced at the N-terminus of the expressed polypeptide. The His-tagged HheB8 could be purified by His-tag-affinity chromatography to apparent homogeneity. The purified HheB8 showed a single band with a molecular mass of approximately 26 kDa on SDS-PAGE (Fig. 3). The specific activity of the recombinant HheB8 toward 1,3-DCP was calculated to be 12.7 ± 1.3 U/mg.

3.3 Characteristics of HheBe

Characterization of HheB8 was carried out using purified enzyme. 1,3-DCP was used to investigate the effects of pH and temperature on the activity of HheB8. The optimal pH for the transformation of 1,3-DCP to ECH was determined to be 9.5, with a obviously decrease in dehalogenation activity as the pH of the buffer moved towards the neutral area, reaching nearly zero level at pH 6.0 (Fig. 4a). The purified enzyme was stable in the pH range from 6.0 to 8.0, retaining over 80% of relative activity after 2 h of incubation (Fig. 4b). An optimal temperature of 40 °C was required for the HheB8 to display its maximum activity with 1,3-DCP as the substrate in Tris–SO_4 buffer. The purified enzyme was stable in a temperature range of 25–35 °C, retaining more than 80% of relative activity. When the temperature increased from 45 to 60 °C, the enzyme activity also decreased sharply (Fig. 5).

Enzyme activity was determined by adding different metal ions with concentration of 2 mM into the reaction solution (Table 1). The presence of calcium and magnesium

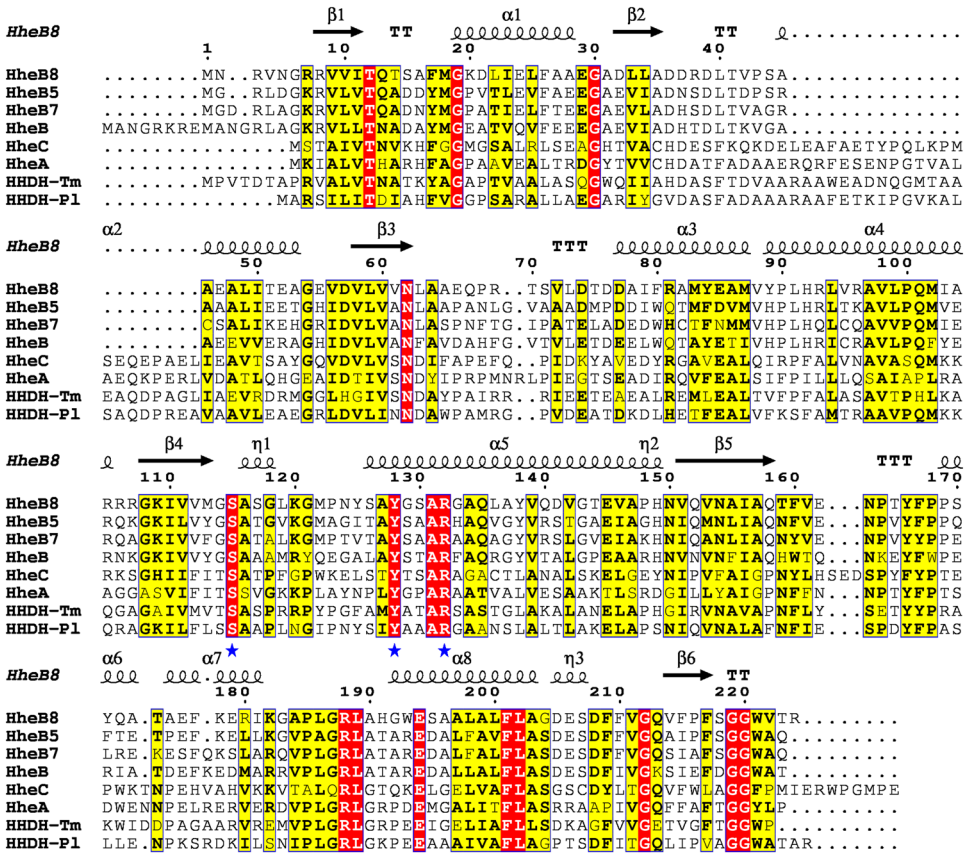

Fig. 1 Sequence alignment of known HHDHs with HheB8. The protein accession numbers are: *Bradyrhizobium erythrophlei* (HheB8, this paper), *Corynebacterium* sp. strain N-1074 (Hhe A, Genbank accession no. BAA14361), *Corynebacterium* sp. strain N-1074 (Hhe B, GenBank accession no. BAA14362), *Agrobaterium radiobater* AD1 (GenBank accession no. AAK92099), *Tistrella mobilis* ZJB1405 (HHDH-Tm, Genbank accession no. AKR76215.1), *Parvibaculum lavamentivorans* DS-1 (HHDH-Pl, Genbank accession no. ABS64560), synthetic construct (HheB5, Genbank accession no. AMQ13562). synthetic construct (HheB7, Genbank accession no. AMQ13564). Yellow and red colours indicate sequence identity and similarity, respectively. The secondary structures are marked above the sequences. The catalytic triad (Ser^{115}, Tyr^{128} and Arg^{132}) are marked by stars

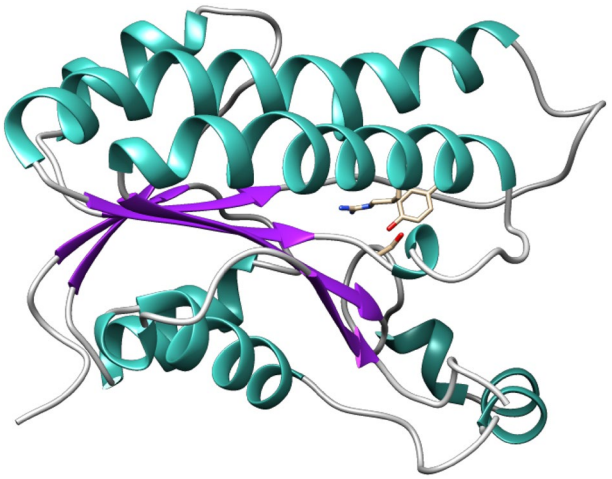

Fig. 2 The overall 3-D structure of HheB8 obtained by homology modeling

ions enhanced the activity of HheBe to 110.5 ± 2.7 and 107.1 ± 1.4%, respectively. However, the other metal ions reduced the enzyme activity. The activity of HheBe was severely inhibited by the Hg^{2+}, Ag^{2+}, partially inhibited by Ni^{2+} and Cu^{2+}, and slightly inhibited by Zn^{2+} and Fe^{2+}. The addition of 2% (v/v) of Tween 80 and Tween 20 induced

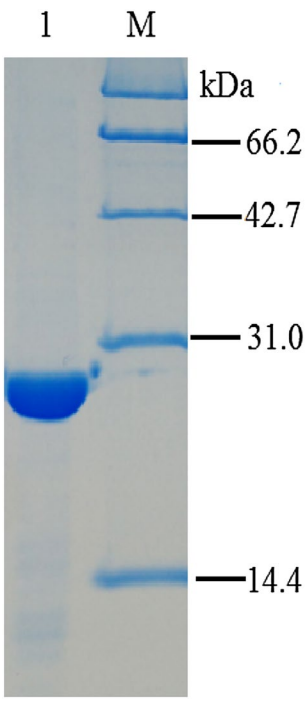

Fig. 3 SDS-PAGE of the purified HheB8 lane M: molecular weight markers; lane 1: purified HHDH

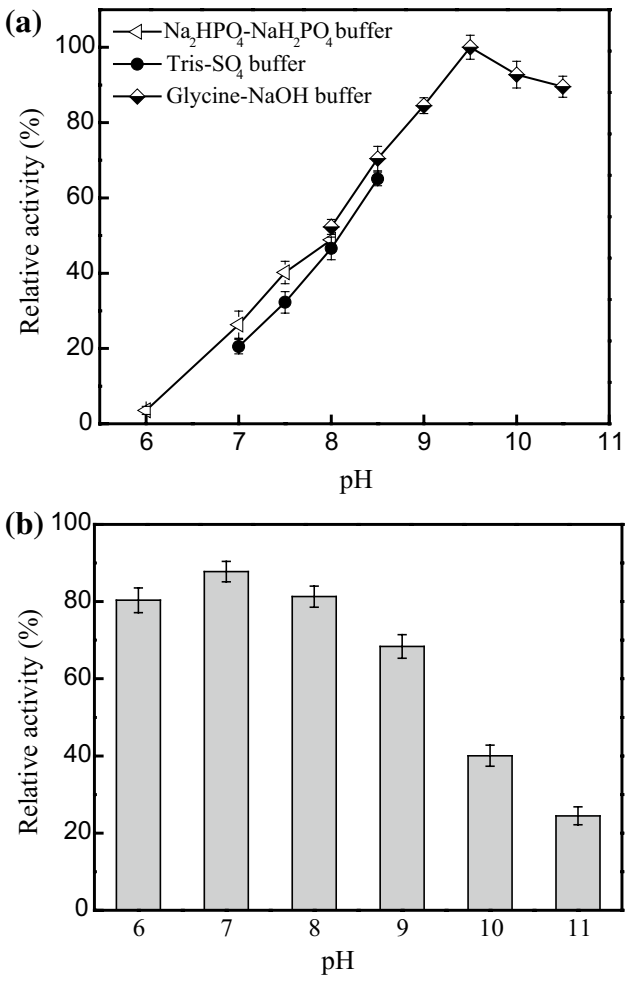

Fig. 4 Effects of pH on the activity (**a**) and stability (**b**) of the purified HheB8. Activities were determined with the substrate 1,3-DCP at temperature 35 °C

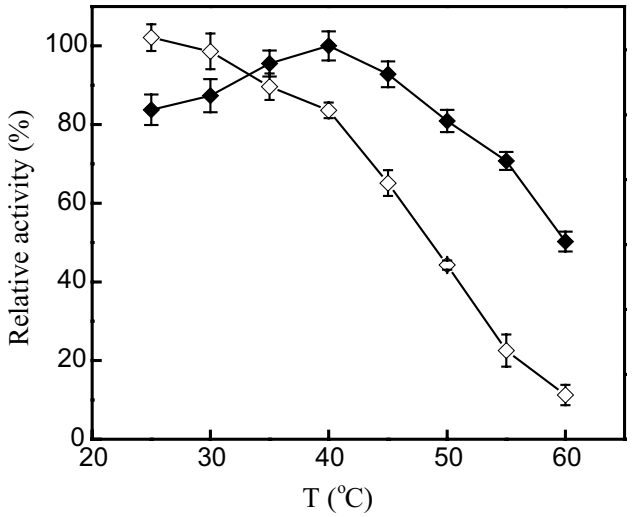

Fig. 5 Effects of temperature on the activity (filled diamond) and stability (open diamond) of the purified HheB8. Activities were determined with the substrate 1,3-DCP at pH 8.0

Table 1 Effects of metal ions and chemical agents on enzyme activity

Reagent	Concentration	Relative activity (%)
Control		100
EDTA	2 mM	96.5 ± 1.9
$AgNO_3$	2 mM	6.4 ± 1.2
$HgCl_2$	2 mM	4.9 ± 2.3
$NiCl_2$	2 mM	47.8 ± 2.5
$CuSO_4$	2 mM	61.3 ± 2.4
$FeCl_2$	2 mM	82.9 ± 2.6
$ZnSO_4$	2 mM	93.8 ± 2.4
$CaCl_2$	2 mM	110.5 ± 2.7
$MgSO_4$	2 mM	107.1 ± 1.4
Trinton X-100	2% (v/v)	97.4 ± 2.2
Tween 20	2% (v/v)	105.5 ± 1.7
Tween 80	2% (v/v)	112.6 ± 2.9

The enzyme activity was measured with the substrate 1,3-DCP after incubating HheB8 with various chemical agents and metal ions at 35 °C for 30 min. The result in the absence of reagents was use as control

the HheB8 activation slightly. The metal chelator EDTA wasn't found to inhibit the activity of enzyme, indicating that HheB8 is not a metalloenzyme.

Values of kinetic constants were determined on the basis of the Lineweaver–Burk plot (1/V vs. 1/[S]) (Fig. 6). The K_m and V_{max} value of HheB8 using 1,3-DCP as the substrate were 13.2 mM and 21.5 μmol/min/mg, respectively.

3.4 Substrate Scope and Enantioselectivity

The substrate specificity of HheB8 toward various halohydrins and epoxides was examined (Tables 2, 3). The relative activities toward the tested compounds are expressed as percentage of that determined with 1,3-DCP and ECH. The highest activity (101.6 U/mg) was observed with 1,3-dibromo-2-propanol. In summary, 1,3-DCP was the best substrate for HheB8 among all the tested chlorinated alcohols. The HheB8 showed low activity on 2-chloro-1-phenylethanol (8.9%), 2,3-dibromo-propanol (5.7%), 2-chloroethanol (2.5%) and 2-bromoethanol (9.4%) corresponding to 1,3-DCP (100%). No activity was detectable on 2,3-DCP. Thus, it was found to be highly active toward α-substituted halohydrins but poorly active toward most of β-substituted derivatives. Activity of HheB8 towards brominated alcohols seems to be higher than that of their chlorinated equivalents, which is not so inexplicable, as the energy of C–Br bond is lower than that of C–Cl. Compared to the experimentally characterized halohydrin dehalogenase $HHDH_{Tm}$, HheB and HheC, the overall activity of HheB8

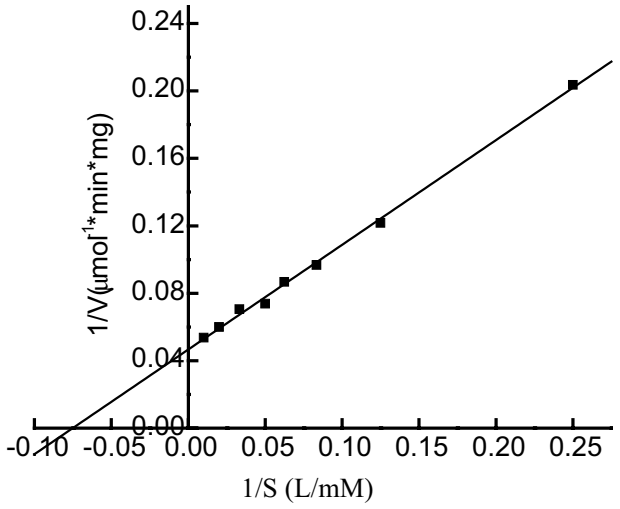

Fig. 6 Determination of K_m and V_{max} of HheB8 on Lineweaver–Burk double reciprocal plots

Table 2 Specific activity and enantioselectivity of HheB8 toward various halohydrins substrates

Substrate	Relative activity[a]	*ee* (%)/configuration
1,3-Dichloro-2-propanol	100	92.3/(*R*)
2,3-Dichloro-propanol	ND[b]	ND
1,3-Dibromo-2-propanol	800 ± 4.4	81.3/(*R*)
2,3-Dibromo-propanol	5.7 ± 1.2	91.0/(*R*)
2-Chloro-1-phenylethanol	8.9 ± 1.7	48.5/(*R*)
2-Chloroethanol	2.5 ± 0.9	–
2-Bromoethanol	9.4 ± 1.5	–

[a]Dehalogenation reaction toward halohydrins was performed in 100 mM Tris–SO_4 buffer (pH 8.0) at 35 °C. All test results were compared to control group without the addition of HheB8. The dehalogenation activity of HheB8 for 1,3-DCP (12.7 μmol/min /mg) was taken as 100%

[b]ND: The enzyme activity was too low to measured

Table 3 Enantioselective ring opening of epoxides with NaN_3 catalysed by HheB8

Substrate	Relative activity	Conversion (%)	*ee* (%)/configuration[a]
Epichlorohydrin	100	68.2	> 99/(*S*)
Epibromohydrin	128 ± 8.6	71.5	> 99/(*S*)
Styrene oxide	15 ± 2.7	86.7	12.6/(*R*)
Phenyl glycidyl ether	65 ± 7.9	76.3	> 99/(*S*)
Benzyl glycidyl ether	87 ± 5.5	82.6	> 99/(*S*)

Value are expressed as percentage of the activity measure with ECH taken as 100% (16.2 μmol/min/mg)

[a]Absolute configuration, meaning the configuration of remaining epoxide after reaction

was lower [16, 19, 20]. The enzyme exhibited up to 11 times lower activity than the most active $HHDH_{Tm}$ and HheB, but up to 6 times higher activity than the least active HheA and $HheA_{Am}$ [18, 21].

The enantioselectivity of the transformation of halohydrins to epoxides was determined by measuring the enantiomeric excess of chiral epoxides after a certain reaction time. The HheB8 displays an enantioselectivity for the transforming prochiral 1,3-DCP, 1,3-dibromo-2-propanol and 2,3-dibromo-2-propanol to (*R*)-ECH (94.2% *ee*), (*R*)-epibromohydrin (81.3% *ee*) and (*R*)-epibromohydrin (91% *ee*). HheB from *Corynebacterium* sp. strain N-1074 gave the high *ee* values for product (*R*)-ECH next to HheB8 [16]. $HHDH_{Tm}$ exhibit opposite stereopreference for 1,3-DCP and 1,3-dibromo-2-propanol transformation, resulted in formation of (*S*)-ECH (60% *ee*) and (*S*)-epibromohydrin (50% *ee*) [19]. The resulting ECH and epibromohydrin catalyzed by HheA and HheC was almost racemic, indicating that enantioselective biotransformation of prochiral halohydrins is not a general characteristic of all HHDHs [15, 17]. We also investigated the enantioselectivity of HheB8 in the dehalogenation of 2-chloro-1-phenylethanol. HheB8 display (*S*)-enantioselectivity toward 2-chloro-1-phenylethanol, while HheC and $HHDH_{Tm}$ wild-type preferentially transforms the (*R*)-enantiomer of this substrate. As far as we know, HheB8 is the most enantioselective of all biochemically characterized HHDHs towards prochiral halohydrins and thus may be attractive for biocatalysis.

To explore substrate specificities of HheB8 in the epoxide ring-opening reaction, their activity and enantioselectivity towards five different epoxides was studied by monitoring epoxide ring-opening with sodium azide by HPLC and GC, respectively. From the results of Table 3 it is concluded that the HheB8 has a broad substrate specificity because all tested epoxides are accepted by this enzyme. The purified HheB8 showed an asymmetric azidolysis toward monosubstituted epoxides at C-1 position with bulky ring such as benzyl glycidyl ether and styrene oxide and with aliphatic chains such as ECH and epibromohydrin. For all tested substrates, except styrene oxide, the (*R*)-enantiomer was converted first. Production of chiral ECH from racemic ECH using HHDH has been reported in the literature. HheC was identified to give *S* enantioselectivity by using sodium azide [11]. In contrast to (*S*)-selective $HheA_{AD2}$ [32], HheB8 could be identified which preferably azidolyzed the (*R*)-enantiomer of styrene oxide, but with low enantioselectivity.

3.5 Synthesis of ECH Using Recombinant *E. coli* (HheB8)

Chiral ECH can be prepared using diverse biological and chemical technologies. By altering the reaction conditions, it was probable to use a single HHDH to enantioselectively

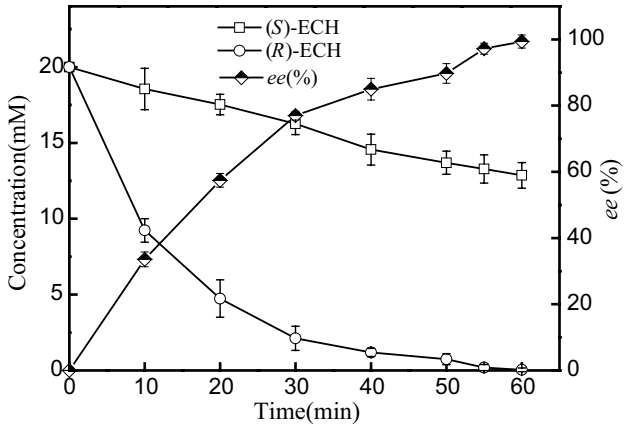

Fig. 7 Enantioselective ring opening of racemic epichlorohydrin by N_3^-←catalyzed by HheB8

produce both enantiomers of ECH. One of the effective ways for obtaining such chiral synthons under mild conditions is the asymmetric azidolysis of racemic ECH using cofactor-independent HHDH. For the initial test, enantioselective azidolysis of racemic ECH was assessed at a concentration of 30 mM with wet cells of *E. coli* BL21(DE3) in 100 mM Tris–SO_4 buffer by addition of NaN_3 (pH 7.5) at 30 °C on a 10 mL-scale. The biotransformation results were analyzed by monitoring the concentrations of (*S*)- and (*R*)-ECH versus time in the reaction mixtures. As shown in Fig. 7, the (*S*)-ECH were azidolyzed slower than (*R*)-ECH, leading to the recovery of the remaining (*S*)-ECH in 33.4% yield and 99% ee (theoretical yield = 50%). Enantioselective azidolysis of racemic ECH has been studied before with HHDHs from other sources. Kinetic resolution of racemic epichlorohydrin (20 mM) by azide-mediated epoxide ring opening using HheC afforded (*R*)-ECH in 39% yield with 99% *ee* [11].

Due to the high yield of the chiral product, great attention has been paid to the production of optically active compounds by enantioselective biotransformation of prochiral starting materials. Stereoselective formation of (*R*)-ECH from 1,3-DCP was performed using whole cells of recombinant *E. coli* in different pH buffer, and effect of substrate loading on the enantioselective dehalogenation of 1,3-DCP was investigated. As shown in Table 4, an increase in the reaction pH resulted in an obvious decrease in the optical purity of (*R*)-ECH from 93.4% at pH 8.5 to 80.1% at pH 10.0. However, the yield of (*R*)-ECH increase as the pH of the reaction solution was changed from 8.0 to 10.0. At low substrate concentration, the yield of (*R*)-ECH increased and the *ee* showed only a small decrease at 1,3-DCP concentrations below 10 mM. The *ee* and yield of (*R*)-ECH respectively decreased from 93.4 and 54.3% to 89.3 and 17.8% as the concentration of 1,3-DCP was increased from 10 to 30 mM.

Table 4 Production of (*R*)-ECH from 1,3-DCP using recombinant *E. coli* (HheB8)

Reaction conditions	(*R*)-ECH (*ee* %)	Yield (%)[a]
pH[b]		
8.0	92.5	44.5
8.5	93.4	54.3
9.0	87.6	59.8
9.5	81.5	61.5
10.0	80.1	76.7
1,3-DCP (mM)[c]		
5	93.0	82.3
10	93.4	54.3
20	90.5	30.1
30	89.3	17.8

[a]The maximum analytical yield is 100%

[b]10 mM 1,3-DCP, 35 °C, 5 min

[c]100 mM Gly–NaOH (pH 8.5), 35 °C

So far, HheB8 seems to be the few HHDH enzyme exhibiting comparably high enantioselectivity in the conversion of 1,3-DCP and racemic ECH, whereas most other HHDHs are either unselective or display only moderate enantioselectivity. These results highlight the potential use of the HheB8 for the production of the chiral epoxides. Ongoing work is focused on the engineering of HheB8 to identify more active HheBe variants with higher activity and enantioselectivity.

4 Conclusions

In summary, a novel HHDH from *B. erythrophlei* has been identified and characterized. The optimal pH and temperature for purified HheB8 towards 1,3-DCP were 9.5 and 40 °C, respectively. Substrate specificity experiments showed that the enantioselectivity profile of HheB8 towards various epoxides and halohydrins is different from other HHDH enzymes. Applying HheBe to kinetic resolution of 30 mM racemic ECH in the presence of an excess of NaN_3, enantiopure (*S*)-ECH could be obtained with more than 99% *ee* and yield of 33.4%. Moreover, (*R*)-ECH was enantioselectively biotransformed from the prochiral 1,3-DCP with a maximum enantiomeric excess of 93.4%. These results highlight the potential use of the HheB8 for the production of the chiral epoxides. Further research will focus on enhancing the activity and enantioselectivity of the recombinant HHDH by genetic modification.

Acknowledgements This work was financially supported by National Natural Science Foundation of China (No. 21606192), China Postdoctoral Science Foundation (No. 2016M601795) and Natural science fund for colleges and universities in Jiangsu Province (No. 16KJB180029).

Compliance with Ethical Standards

Conflict of interest The authors declared that they have no conflicts of interest to this work.

References

1. Schallmey A, Schallmey M (2016) Appl Microbiol Biotechnol 100:7827
2. You ZY, Liu ZQ, Zheng YG (2013) Appl Microbiol Biotechnol 97:9
3. Castro CE, Bartnicki EW (1968) Biochemistry 7:3213
4. Higgins TP, Hope SJ, Effendi AJ et al (2005) Biodegradation 16:485
5. Ma SK, Gruber J, Davis C et al (2010) Green Chem 12:81
6. Chen SY, Yang CX, Wu JP et al (2013) Adv Synth Catal 355:3179
7. Zou SP, Zheng YG, Du EH et al (2014) J Biotechnol 188:42
8. Jin HX, Liu ZQ, Hu ZC et al (2013) Biochem Eng J 74:1
9. Seisser B, Lavandera I, Faber K et al (2007) Adv Synth Catal 349:1399
10. Xue F, Liu ZQ, Zou SP et al (2014) Process Biochem 49:409
11. Spelberg JHL, Tang LX, Kellogg RM et al (2004) Tetrahedron Asymmetry 15:1095
12. Assis HMS, Bull AT, Hardman DJ (1998) Enzym Microb Technol 22:545
13. Kasai N, Tsujimura K, Unoura K et al (1992) J Ind Microbiol Biotechnol 10:37
14. Yonetani R, Ikatsu H, Miyake-Nakayama C et al (2004) J Health Sci 50:605
15. Nagasawa T, Nakamura T, Yu F et al (1992) Appl Microbiol Biotechnol 36:478
16. Nakamura T, Nagasawa T, Yu FJ et al (1994) Appl Environ Microbiol 60:1297
17. Liu ZQ, Gao AC, Wang YJ et al (2014) J Ind Microbiol Biotechnol 41:1145
18. Xue F, Liu ZQ, Wan NW et al (2014) Appl Biochem Biotechnol 174:352
19. Xue F, Liu ZQ, Wang YJ et al (2015) J Mol Catal B 115:105
20. Vlieg JETV., Tang LX, Spelberg JHL et al (2001) J Bacteriol 183:5058
21. Vandenwijngaard AJ, Reuvekamp PTW, Janssen DB (1991) J Bacteriol 173:124
22. Schallmey M, Koopmeiners J, Wells E et al (2014) Appl Environ Microbiol 80:7303
23. Wan NW, Liu ZQ, Huang K et al (2014) RSC Adv 4:64027
24. Koopmeiners J, Halmschlag B, Schallmey M et al (2016) Appl Microbiol Biotechnol 100:7517
25. Bradford MM (1976) Anal Biochem 72:248
26. Laemmli UK (1970) Nature 227:680
27. Gasteiger E, Gattiker A, Hoogland C et al (2003) Nucleic Acids Res 31:3784
28. Robert X, Gouet P (2014) Nucleic Acids Res 42:320
29. Watanabe F, Yu F, Ohtaki A et al (2015) Proteins: Struct Funct Bioinf 83:2230
30. Zhao J, Chu YY, Li AT et al (2011) Adv Synth Catal 353:1510
31. Chen CS, Fujimoto Y, Girdaukas G et al (1982) J Am Chem Soc 104:7294
32. Tang LX, Zhu XC, Zheng HY et al (2012) Appl Environ Microbiol 78:2631

Affiliations

Feng Xue[1,2] · Jian Gao[1] · Li Zhang[1] · Han Li[1] · He Huang[2]

✉ Jian Gao
gaojian@ycit.edu.cn

✉ He Huang
biotech@njtech.edu.cn

Feng Xue
coldsun_xf@163.com

Li Zhang
zllz@ycit.cn

Han Li
lihan620@ycit.cn

[1] School of Marine and Bioengineering, Yancheng Institute of Technology, Yancheng 224051, People's Republic of China

[2] College of Pharmaceutical Science, Nanjing Tech University, Nanjing 210009, People's Republic of China